International Journal of Architectural, Civil and Construction Sciences
ISSN: 2415-1734
Vol:10, No:10, 2016

Seismic Fragility Curves for Shallow Circular Tunnels under Different Soil Conditions

Siti Khadijah Che Osmi, Syed Mohd Ahmad

***Abstract*—**This paper presents a methodology to develop fragility curves for shallow tunnels so as to describe a relationship between seismic hazard and tunnel vulnerability. Emphasis is given to the influence of surrounding soil material properties because the dynamic behaviour of the tunnel mostly depends on it. Four ground properties of soils ranging from stiff to soft soils are selected. A 3D nonlinear time history analysis is used to evaluate the seismic response of the tunnel when subjected to five real earthquake ground intensities. The derived curves show the future probabilistic performance of the tunnels based on the predicted level of damage states corresponding to the peak ground acceleration. A comparison of the obtained results with the previous literature is provided to validate the reliability of the proposed fragility curves. Results show the significant role of soil properties and input motions in evaluating the seismic performance and response of shallow tunnels.

***Keywords*—**Fragility analysis, seismic performance, tunnel lining, vulnerability.

I. Introduction

UNDERGROUND structures are classified as complex engineered structures that require detailed analysis and design. Tunnels, for instance, are massively constructed as transportation infrastructures and utility network, especially in urban environments where space is very limited. Although the construction cost of underground structures is very expensive, such structures are as the less vulnerable structures during earthquakes compared to aboveground structures [1]. However, due to severe damage experienced on the several Dakai subway stations after being attacked by the Hyogoken-Nambu earthquake on 17 January 1995, experience suggests that tunnels become vulnerable during an earthquake event. In fact, any instability of the structure will provide some level degree of damage that may highly detrimental the overall performance of the network (e.g. [2]–[4]). Considering their utmost importance to the public safety that cannot be compromised, engineering practitioners have become more aware of the safety of such structures during an event of an earthquake because if the structures are damaged, the repairing works are not only costly and time-consuming but it is also difficult to carry out the rescue works. However, a very limited amount of studies has been carried out to study and understanding the dynamic performance of tunnels under such unpredictable extreme hazards. In view of the importance to enhance the resilience of these structures, the overall aims of the study are drawn in order to evaluate the probabilistic future performance of tunnels during an earthquake event. This can be done by constructing the fragility curves as a representation of a conditional probability of a structure to endure a specific damage level when subjected to a given hazard. Recently, [6] developed methodologies for the construction of numerically derived fragility curves for tunnels (circular and rectangular sections) in alluvial deposits. They investigated the seismic response of shallow tunnel under quasi-static 2D plane-strain conditions, where the induced seismic ground deformations calculated through 1D free field analysis are applied at the boundaries of the soil-tunnel system. They compared the numerically derived curves with the previous empirical curves and highlighted that the important role of soil conditions and typology of the tunnel in modifying the response of the tunnel lining. Along these lines, it is strongly suggested that the tunnels behave differently due to uncertainties of soil, structure and induced seismic hazard. Instead of performing 2D analysis, the 3D nonlinear time history analyses are considered to evaluate the seismic dynamic response of a circular shallow tunnel. Particular emphasis is given to the influence of surrounding soil material properties because the dynamic behaviour of the tunnel mostly depends on it. The tunnel models are assumed to be buried in four homogenous ground media (i.e. [7]) ranging from stiff to soft soils and are expected to experience a strong earthquake ground motion.

This paper is intended to tackle several important shortcomings of the 2D analysis on evaluating the seismic response of tunnels and to highlight the effect of soil material properties of soil in describing the interaction.

Siti Khadijah Che Osmi, PhD candidate, and Syed Mohd Ahmad, Lecturer, are with the School of Mechanical, Aerospace and Civil Engineering, University of Manchester, United Kingdom, (e-mail: sitikhadijah.cheosmi@postgrad.manchester.ac.uk, mohammed.ahmad.syed@manchester.ac.uk).

II. Methodology

The proposed procedure for the derivation of fragility curves of the 3D tunnel models subjected to strong ground shaking is depicted in Fig. 1. This procedure has been developed by neglecting the 1D equivalent linear analysis of the soil profiles which usually conducted to estimate the dynamic properties of layered soil as presented by the previous studies (see [6], [8]-[10]). Instead, in this study, the material properties of the homogeneous soil profiles were taken as suggested in [11]. The representative soil-tunnel models are developed to describe the specific geometry and characteristic of the proposed models, in which consideration has been made for the uncertainties of soil parameters.

In this paper, the dynamic response of the tunnels was evaluated by performing 3D nonlinear time history analyses using the sophisticated finite element software, Midas GTS

NX. The software is widely used for various geotechnical engineering and tunnel engineering problems. Prior to the nonlinear analyses, the representative soil-tunnel models are developed to investigate the seismic responses of the tunnel models subjected to a given transversal loading. In particular, the four homogenous soil profiles and five seismic input motions are used to highlight the influence of soil material properties on the seismic fragility of the shallow tunnel. The fragility curves are constructed as a function of damage level and the type of seismic excitation. This approach allows an evaluation of fragility curves for tunnels with respect to the distinctive features of tunnel's geometries, input motion characteristics, and soil properties.

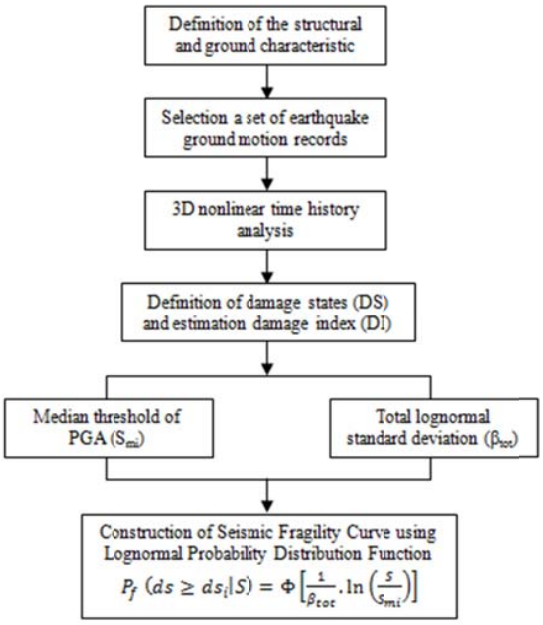

Fig. 1 Procedure for numerically derived fragility curves

TABLE I
DEFINITION OF DAMAGE STATES FOR TUNNEL LINING [6]

Damage state (DS)	Range of damage index (DI)	Central value of damage index
DS1. Minor/slight	$1.0 < M/M_{Rd} \leq 1.5$	1.25
DS2. Moderate	$1.5 < M/M_{Rd} \leq 2.5$	2.00
DS3. Extensive	$2.5 < M/M_{Rd} \leq 3.5$	3.00
DS4. Collapse	$M/M_{Rd} > 3.5$	-

A. Damage States

The damage states as described in Table I were adopted in the present study as an approach to evaluate the seismic performance of the proposed tunnels models. Due to lack of references available for definition of damage index for tunnels, in this present study, the damage index (DI) is defined as the ratio between the actual (M) and capacity (M_{Rd}) bending moment of the tunnel cross section [6]. In particular, the tunnel is assumed to behave as an elastic beam and will be deformed due to imposed seismic waves propagating perpendicular to the tunnel axis [5]. M is calculated as the combination of static and seismic loads using the Midas GTS NX finite element software [12], while M_{Rd} is estimated through a section analysis [13] accounting for the seismic induced axial forces (N) and bending moment (M). Many studies suggest that four damage states (i.e. minor, moderate, extensive and complete) of tunnel lining are considered due to ground shaking.

B. Fragility Curves Parameters

As refer to (1), most of the available fragility curves (i.e. [6], [14], [15]) are usually described by a lognormal probability distribution function:

$$P_f\ (ds \geq ds_i|S) = \Phi\left[\frac{1}{\beta_{tot}}.\ln\left(\frac{S}{S_{mi}}\right)\right] \quad (1)$$

where $P_f(\cdot)$ is the probability of exceeding a particular damage state, ds, for a given seismic intensity level defined by the earthquake intensity measure S (e.g. peak ground acceleration (PGA)), S_{mi} is the median threshold value of S required to cause the i^{th} DS, and β_{tot} is the total lognormal standard deviation. According to (1), the development of fragility curves requires the definition of two critical parameters, $S_{mi,}$ and β_{tot}.

Thus, the lognormal standard deviation (β_{tot}) is estimated as the root of the sum of the squares of the component dispersions as described in (2). The value of β_{tot} is largely depended on three primary sources of uncertainty [15], namely; the definition of DS (β_{ds}), the response and resistance (capacity) of the element (β_C), and the earthquake input motion (β_D).

$$\beta_{tot} = \sqrt{{\beta_{ds}}^2 + {\beta_C}^2 + {\beta_D}^2} \quad (2)$$

As mentioned earlier, in order to determine total lognormal standard deviation (β_{tot}), two crucial parameters β_D and S_{mi} have to be estimated first. Considering the lack of more rigorous estimation, the parameters β_{ds} and β_C are taken as 0.4 and 0.3, respectively [6], [15]. The last source of uncertainty, associated with seismic demand, is described by the average standard deviation of the damage indices that have been calculated for different input motions at each level of PGA.

III. NUMERICAL MODELLING

The seismic response of the tunnel models was evaluated through 3D nonlinear time history analyses, subjected to five seismic ground motion which applied in the transverse direction of tunnel axis. The analyses were performed using the Midas GTS NX finite element software [12], in which the representative soil-tunnel model as depicted in Fig. 2. The model with dimension 150m x 75m x 60m (*xyz*) was chosen to avoid the effects of boundary condition to the numerical results [16].

The tunnel lining is composed of 10m diameter, 0.5m thick lining, and is buried at 25m overburden depth which measures from the ground surface up to the crown of tunnel lining. The behaviour of the tunnel lining was assumed to be linear elastic beam and was simulated as shell elements. In total, for one

particular model required the total number of nodes, elements, DOFs and EQNs are 4904, 9539, 20043, and 18945 respectively. As shown in Fig. 2, the adopted mesh dimension and element size was adopted to ensures the efficiency of reproduction of all the waveforms for the whole frequency of the simulated tunnel models [7].

Several boundary conditions are considered as recommended by the previous literature [17]. In this present study, the surface of soil was assumed to be flat and free from loadings, while fixed boundary condition at the bottom of the homogenous soil which overlaying the rigid bedrock, was assumed at *x*, *y* and *z*-axes of the tunnel model. However, the sides boundaries of the soil are allowed to move on *x* and *z* but fixed on *y*-axes. The input motion is introduced at the base boundary in terms of acceleration time history.

A. Modeling of Materials

Considering the uncertainties of the geological condition, four homogeneous ground properties adopted in this study are ranging from stiff to soft soils as described in Table II. The selected geometrical and material properties of tunnel lining was taken from the available previous literature review (i.e. [11]) are listed in Table III.

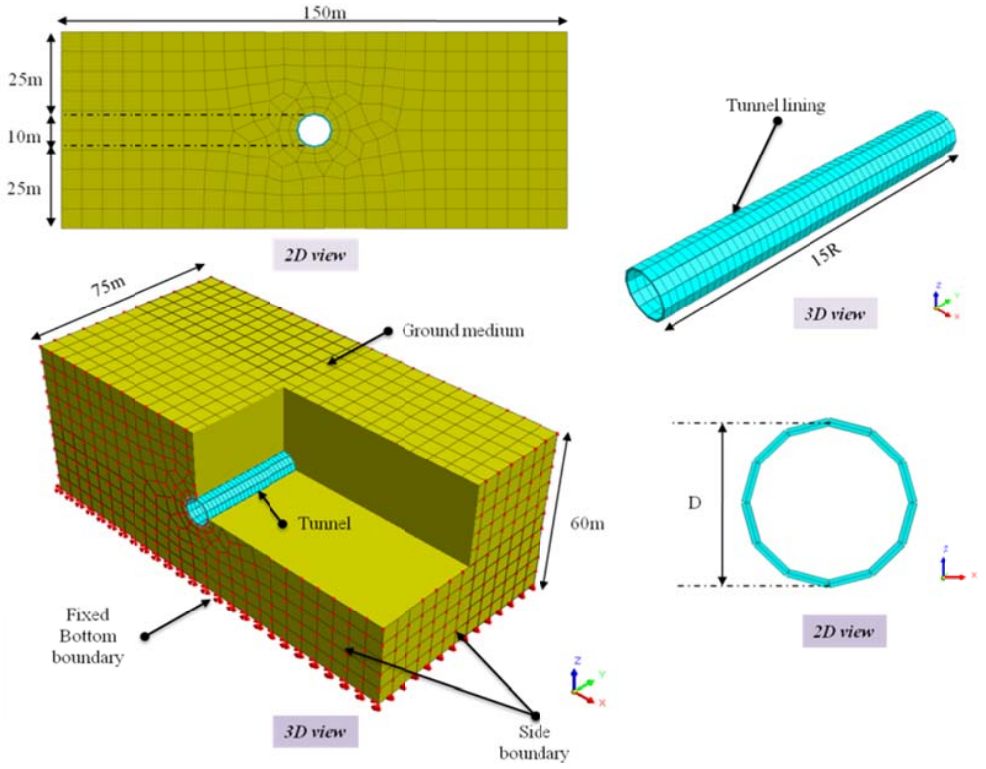

Fig. 2 Geometry, meshing and boundary conditions of the soil-tunnel system

TABLE II
MATERIAL PROPERTIES OF THE SOIL MODELS [7], [19]

MAIN PROPERTIES	TYPES OF SOIL			
	Dense Sand	Loose Sand	Stiff Clay	Soft Clay
Element type	3D Solid	3D Solid	3D Solid	3D Solid
Material model	Modified Mohr-Coulomb	Modified Mohr-Coulomb	Mohr-Coulomb	Mohr-Coulomb
Unit weight [kN/m^3]	20	17	17	16
Modulus of elasticity, E [kN/m^2]	15 x 10^4	10 x 10^4	2.5 x 10^4	1.0 x 10^4
Poison ratio, ν	0.3	0.3	0.3	0.3
Cohesion, c [kN/m^2]	20	10	10	10
Friction angle, φ [^{o}]	36	30	18	17.5
At-rest earth pressure coefficient , K_0	0.4	0.5	1.0	1.0
Damping ratio	0.05	0.05	0.05	0.05

B. Modeling of Seismic Loading

Five real records of earthquake time histories as summarised in Table IV were considered as input motion in outcrop condition for the 3D nonlinear time history analyses at the transverse direction of the tunnel axis (*x*-axis). The unscaled strong ground acceleration time histories was

selected in order to calculate the response of the soil-tunnel systems for increasing levels of seismic intensity. The selected records for seismic loadings was taken from two sources; PEER Ground Motion Database [18] and the default values available in the Midas program.

TABLE III
MATERIAL PROPERTIES OF THE TUNNEL MODELS [20]; [21]

Lining Main Properties	Value
Element type	2D Shell
Material model	Elastic
Unit weight [kN/m^3]	24
Modulus of elasticity, E [kN/m^2]	35 x 10^6 (C40/50)
Poison ratio, ν	0.2
Diameter, d [m]	10
Radius, r [m]	5
Thickness of lining, t [m]	0.5
Area of tunnel lining (per unit width), A_l [m^2/m]	0.5
Moment inertia of the lining (per unit width), I [m^4/m]	0.01042
Damping ratio	0.05

TABLE IV
SELECTED REAL EARTHQUAKE RECORDS [12], [22]

EARTHQUAKE NAME	Year	PGA (g)	Duration (s)
Kobe, Japan	1995	0.452	32.00
Hyougoken South, Japan	1995	0.781	30.00
Northridge, Los Angeles , USA	1994	0.6047	59.98
Loma Prieta, California, USA	1989	0.288	39.99
El Centro, California, USA	1979	0.777	37.68

IV. COMPARISON OF NUMERICAL RESULTS

A. Displacement and Structural Forces

In the present study, the influence of the most critical parameters affecting the structural response is determined and critically discussed through parametric analysis. The effect on soil material properties on the obtained displacement and structural forces of the investigated tunnel models is summarized in Figs. 3-6.

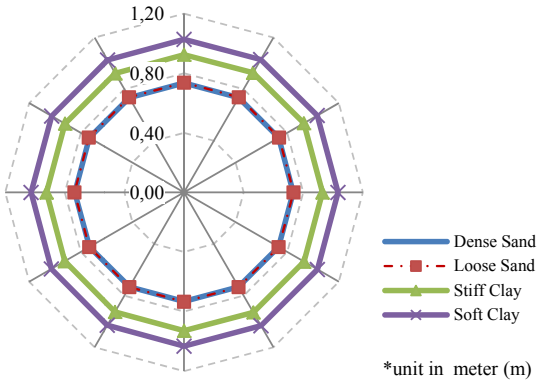

Fig. 3 The maximum transverse displacement distribution in the lining subjected to the Hyougoken earthquake record

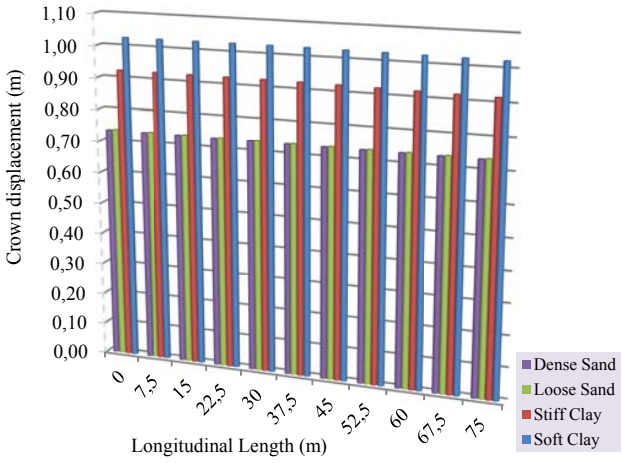

Fig. 4 The maximum longitudinal crown displacement of liner subjected to the Hyougoken earthquake record

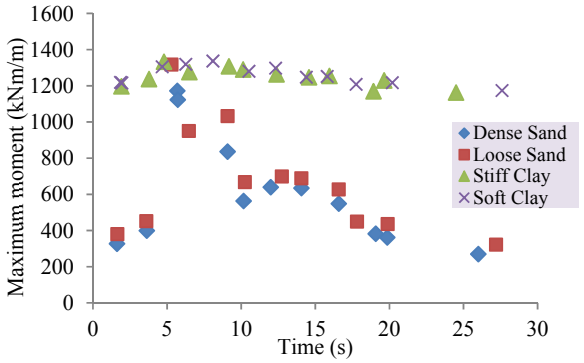

Fig. 5 The overall maximum bending moments of the shell element subjected to the Hyougoken earthquake record

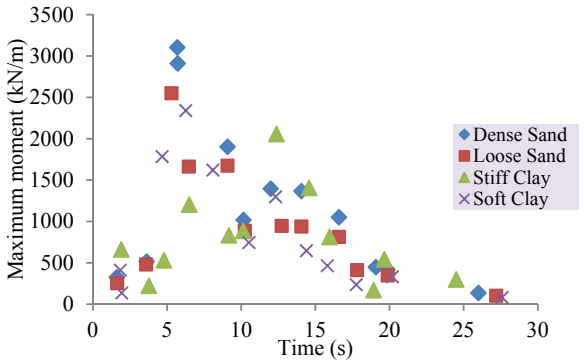

Fig. 6 The overall maximum axial forces of the shell element subjected to the Hyougoken earthquake record

The obtained numerical results are compared to four different types of soil material properties. It is found that the both the transverse and longitudinal displacement of the liner in Soft Clay is higher than the values obtained for other types of soil properties (Figs. 3 and 4). Meanwhile, in Figs. 5 and 6,

it is noted that high level of PGA resulted to the higher value of seismic induced structural forces (i.e. axial force and bending moment). Although, this parameter was not been the only parameter that attributed to the failure of the lining [23] because the response and performance of the tunnels are depending on various uncertainties factors as suggested by [24], [25] (i.e. typology of tunnels, geological condition, and earthquake parameters).

B. Derivation of Fragility Curves

Prior to the derivation of fragility curves, two fragility functions: S_{mi} and β_{tot} were calculated for each type of soil. The example of evolution graph with the function of damage index and the PGA is illustrated in Figs. 7 (a) and (b). The relationship of damage index and the PGA is described by the solid trendline and the input dataset is fitted by an average linear regression analysis. The medium threshold value of the PGA (S_{mi}) for minor, moderate and extensive damage state can be estimated using the equation of linear regression. The graph is constructed by considering the natural logarithm of the damage index (lnDI) as the dependent variable and PGA as the independent variable.

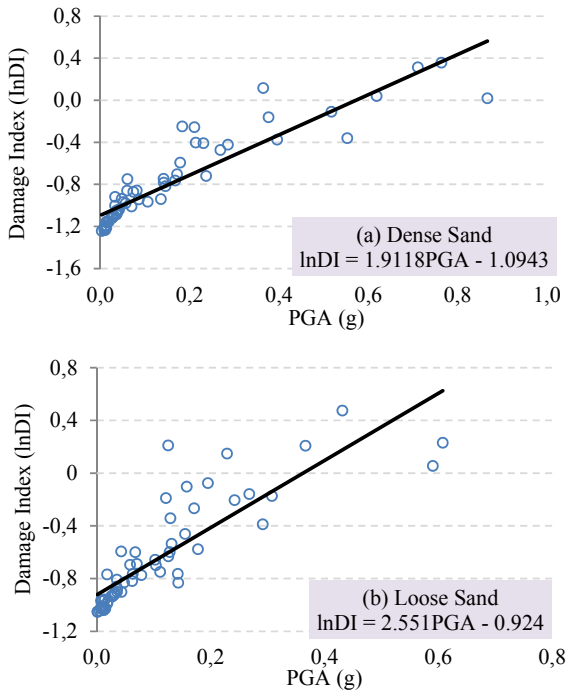

Fig. 7 The example of the evolution of damages with PGA at the ground surface for circular tunnel model buried in (a) Dense Sand and (b) Loose Sand

In particular, the set of fragility curves derived for dense sand, loose sand, stiff clay and soft clay are depicted in Figs. 8-11. The derived seismic fragility curves describe the percentage probability of exceeding different damage states for a given value of ground shaking (i.e. PGA). The curves are estimated using the lognormal probability distribution function as provided in (1). A clear trend between percentage probability of damage and PGA was observed for all types of soil. The fragility curves are derived based on the extrapolation values of the computation results. As can be seen, the higher percentage of minor damage state is expected to occur in each type of soil compared to the moderate and extensive damage states. Similarly, the rate of damage increases with the increment of PGA, while the vulnerability of tunnel model is gradually increasing from soil type dense sand to soft clay. The results could be attributed from the different value of soil material properties such as modulus elasticity, Poisson's ratio, cohesion and friction angle [6], [26]. It is noted that soft clay soil will suffer high probability of damage compared to other types of soils.

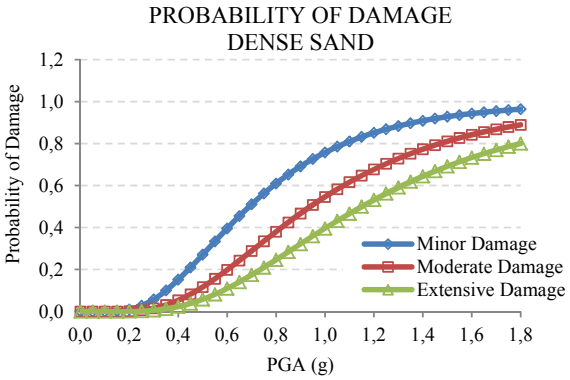

Fig. 8 Fragility curves of circular tunnel for dense sand

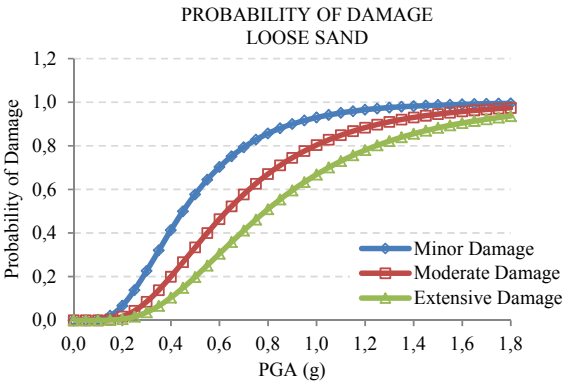

Fig. 9 Fragility curves of circular tunnel for loose sand

In comparison, the derived fragility curves are predicted to experience a higher percentage of minor damage compared to the previous fragility curves (Fig. 12). Overall, it can be seen that a good agreement is achieved in the for all comparative fragility analysis especially for the fragility curve of clay medium. This can be attributed to the input parameters of soil material properties such as stiffness and damping of the soils. The obtained results also revealed that better agreement in the seismic tunnel responses is recorded although a different type of analysed conditions was adopted by the researchers (3D nonlinear time history versus 2D quasi-static). In fact, the proposed 3D models provided a better representation for

analysing complex structure like tunnels, and not only accounted the effect of SSI, but it also produced acceptable results for nonlinear time history analysis [16]. In addition, the definition of damage index, damage states, and beta values also can alter the obtained results. These assumptions are made due to the complex nature of the seismic fragility problem.

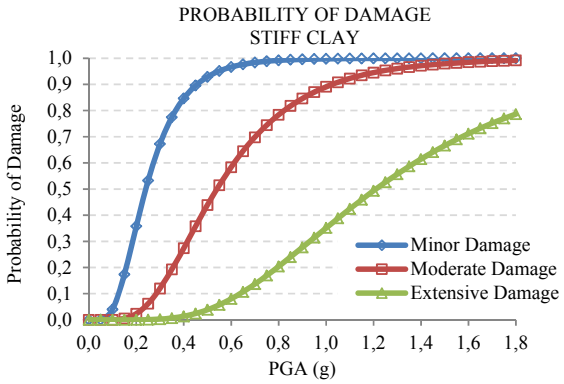

Fig. 10 Fragility curves of circular tunnel for stiff clay

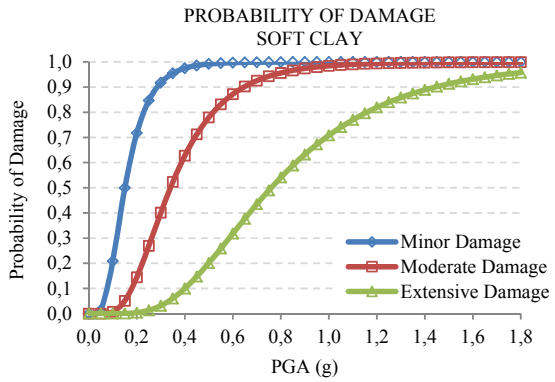

Fig. 11 Fragility curves of circular tunnel for soft clay

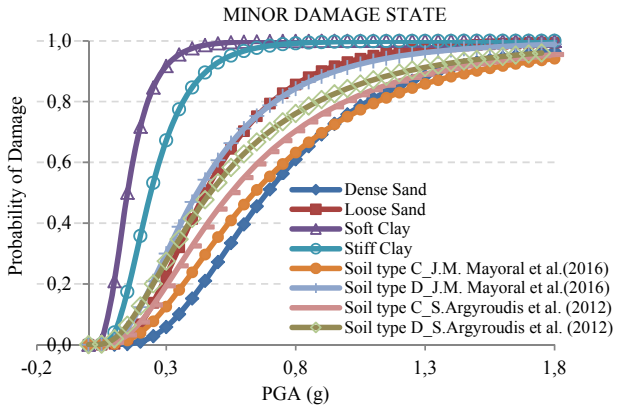

Fig. 12 Comparison of analytical fragility curves for Minor Damage State

V. Conclusion

The comprehensive methodologies for the derived seismic fragility curves of the proposed shallow tunnel models embedded in four homogenous soil medium presented herein refer to the future probabilistic performance experienced by the structure when subjected to transversal seismic loading. In particular, the proposed methodology presented and applied to a representative soil-tunnel system. Tunnel dynamic response is evaluated through 3D nonlinear time history dynamic analyses, for increasing levels of seismic intensity in the transverse direction of tunnel axis. Critical analysis has been presented about the current methods of analysis, structural typology, ground motion characteristics, the effect of soil conditions and associated uncertainties on the tunnel integrity. The damage state thresholds are defined based on the exceedance of the lining capacity due to the development of lining forces. The fragility curves are estimated in terms of peak ground acceleration at the ground surface, based on the evolution of damage with increasing earthquake intensity. The results are compared and validated with available literature study.

It was found that the surrounding soil plays an important role in evaluating the future performance of the tunnel. The curves modified due to different soil condition, where the tunnel that buried in high stiffness behaves better than the lower ones. The results show that there is a strong relation between the soil condition and the seismic response of the tunnels. The lowest percentage probability of tunnel damage occurs in well-constructed tunnels in good ground conditions, especially in stiff soil. Results denote the significant role of soil condition and input motions in evaluating the performance and response of the tunnel. It is interesting to remark that soil with high strength (stiffness) which is stiff soil perform better compared to the typical soft soil.

It can be concluded that the 3D nonlinear time history analysis provides a better representation and acceptable result in evaluating the seismic behaviour and response of the complex structure like tunnels, with consideration of soil-structure interaction. In fact, the derived fragility curves can be readily adopted as a guide for preliminary assessment of tunnel response against different seismic scenarios in typical soil profiles. However, critical analyses are required to ensure that the proposed fragility curve is reliable to cover a major aspect of the study and might be useful to provide new knowledge for risk assessment and loss estimation.

Acknowledgment

Siti Khadijah Che Osmi gratefully acknowledges the financial support of the Ministry of Education Malaysia (MOE) and National Defence University of Malaysia (NDUM) to conduct the research at the University of Manchester, UK.

References

[1] Y. M. a. Hashash, J. J. Hook, B. Schmidt, and J. I-Chiang Yao, "Seismic design and analysis of underground structures," *Tunn. Undergr. Sp. Technol.*, vol. 16, no. 4, pp. 247–293, Oct. 2001.

[2] A. Brito and M. Lopes, "New methodology for the Seismic Design of Large Underground Structures," in *15 WCEE LISBOA 2012*, 2012.
[3] J. H. Wood, "Earthquake Design of Rectangular Underground Structures," *Bull. New Zeal. Soc. Earthq. Eng.*, vol. 40, no. 1, pp. 1–6, 2007.
[4] H. Huo, A. Bobet, G. Fernández, and J. Ramírez, "Load Transfer Mechanisms between Underground Structure and Surrounding Ground: Evaluation of the Failure of the Daikai Station," *J. Geotech. Geoenvironmental Eng.*, vol. 131, no. 12, pp. 1522–1533, 2005.
[5] Y. M. a. Hashash, J. J. Hook, B. Schmidt, and J. I-Chiang Yao, "Seismic design and analysis of underground structures," *Tunn. Undergr. Sp. Technol.*, vol. 16, no. 4, pp. 247–293, Oct. 2001.
[6] S. A. Argyroudis and K. D. Pitilakis, "Seismic fragility curves of shallow tunnels in alluvial deposits," *Soil Dyn. Earthq. Eng.*, vol. 35, pp. 1–12, 2012.
[7] B. Maidl, M. Thewes, and U. Maidl, *Handbook of Tunnel Engineering II: Basics and Additional Services for Design and Construction*. Wiley, Ernst and Sohn, 2014, pp. 25–29.
[8] S. Argyroudis, G. Tsinidis, F. Gatti, and K. Pitilakis, "Seismic fragility curves of shallow tunnels considering SSI and aging effects," in *2nd Eastern European Tunnelling Conference "Tunnelling in a Challenging Environment,"* 2014, pp. 1–10.
[9] S. Argyroudis and A. M. Kaynia, "Fragility Functions of Highway and Railway Infrastructure," in *SYNER-G: Typology Definition and Fragility Functions for Physical Elements at Seismic Risk*, vol. 27, S. Argyroudis and A. M. Kaynia, Eds. Dordrecht: Springer Netherlands, 2014, pp. 299–326.
[10] K. Pitilakis, S. Argyroudis, K. Kakderi, P. Gehl, N. Desramaut, B. Khazai, A. Yakut, A. M. Kaynia, J. Johansson, M. Fardis, F. Karantoni, P. Askouni, F. Lyrantzaki, A. Papailia, G. Tsionis, H. Crowley, M. Colombi, and R. Monteiro, "Guidelines for deriving seismic fragility functions of elements at risk: Buildings, lifelines, transportation networks and critical facilities (SYNER-G Reference Report 4)," 2013.
[11] A. Amorosi and D. Boldini, "Numerical modelling of the transverse dynamic behaviour of circular tunnels in clayey soils," *Soil Dyn. Earthq. Eng.*, vol. 29, pp. 1059–1072, 2009.
[12] Midas GTS NX, "Midas GTS NX User Manual: Chapter 6. Analysis," *Midas Family Package*. pp. 401–442, 2012.
[13] Oasys Ltd, "Adsec: Version 8.2." 2014.
[14] M. Shinozuka, M. Q. Feng, J. Lee, and T. Naganuma, "Statistical Analysis of Fragility Curves," *J. Eng. Mech.*, vol. 126, no. December, pp. 1224–1231, 2000.
[15] National Institute of Building Sciences (NIBS), "Multi-hazard Loss Estimation Methodology Earthquake Model: HAZUS® MH MR4 Technical Manual," Washington, D.C, 2004.
[16] G. D. Hatzigeorgiou and D. E. Beskos, "Soil–structure interaction effects on seismic inelastic analysis of 3-D tunnels," *Soil Dyn. Earthq. Eng.*, vol. 30, no. 9, pp. 851–861, Sep. 2010.
[17] The British Tunnelling Society (BTS) and Institution of Civil Engineers (ICE), *Tunnel Lining Design Guide*. Thomas Telford Books, 2004, pp. 100–113.
[18] P. E. E. R. C. PEER, "PEER Ground Motion Database," *Shallow Crustal Earthquakes in Active Tectonic Regimes, NGA-West2*, 2013. (Online). Available: http://ngawest2.berkeley.edu/.
[19] BS EN 1998-1:2004 and T. E. S. E. 1998-1:2004 has status of a B. S. European Committee for Standardization, *Eurocode 8: Design of structures for earthquake resistance BS EN 1998-1:2004*, vol. 3. 2004.
[20] Y. M. a. Hashash, D. Park, and J. I.-C. Yao, "Ovaling deformations of circular tunnels under seismic loading, an update on seismic design and analysis of underground structures," *Tunn. Undergr. Sp. Technol.*, vol. 20, no. 5, pp. 435–441, Sep. 2005.
[21] N. Iranisarand, "Effect of Vertically Propagating Shear Waves on Seismic Behavior of Circular Tunnels," *15th World Conf. Earthq. Eng.*, vol. 2014, 2012.
[22] Pacific Earthquake Engineering Research (PEER) Center, "PEER Ground Motion Database," 2014. (Online). Available: http://ngawest2.berkeley.edu/.
[23] American Lifelines Alliance (ALA), "Seismic Fragility Formulations for Water Systems: Part 1 - Guideline, ASCE-FEMA, Reston," 2001.
[24] N. G. Owen and R. E. Scholl, "Earthquake Engineering of Large Underground Structures," 1981.
[25] S. Sharma and W. R. Judd, "Underground opening damage from earthquakes," *Eng. Geol.*, vol. 30, pp. 263–276, 1991.
[26] J. M. Mayoral, S. Argyroudis, and E. Castañon, "Vulnerability of floating tunnel shafts for increasing earthquake loading," *Soil Dyn. Earthq. Eng.*, vol. 80, pp. 1–10, 2016.